Synthesis Glycine-Modulated Metal Organic Framework Cr-PTC-Gly for Synergetic Methylene Blue Adsorption and Photodegradation under Visible Light Irradiation

Adawiah Adawiah[1], Risma Nur Fitria[2], Nanda Saridewi[3]*, Wulandari Oktavia[2], Farhan Maulana Azhar[2], Muhammad Shofyan Gunawan[2], Sri Komala[2]

[1]Integrated Laboratory Centre, Faculty of Science and Technology UIN Syarif Hidayatullah Jakarta
Tangerang Selatan 15412, Indonesia
[2]Chemistry Department, Faculty of Science and Technology UIN Syarif Hidayatullah Jakarta
Tangerang Selatan 15412, Indonesia
[3]Chemistry Education Department, Faculty of Tarbiya and Teaching Sciences,
UIN Syarif Hidayatullah Jakarta,Tangerang Selatan 15412, Indonesia

*Corresponding author email: nanda.saridewi@uinjkt.ac.id

ABSTRACT. The glycine-modulated metal-organic framework (MOF) Cr-PTC-Gly was successfully synthesized for methylene blue elimination application. The Fourier Transform Infra-Red (FTIR) characterization showed the stretching vibration N-H at 2034 cm^{-1}. The bands at 1506 and 1406 cm^{-1} are asymmetric and symmetric stretching vibrations (-COO) bound to Cr^{3+} ions and 3118 cm^{-1} of the hydroxyl (OH) functional group of H$_2$O bound to the Cr^{3+} ion. The band gap energy of MOF Cr-PTC-Gly is 1.9 eV. The XRD analysis showed that MOF Cr-PTC-Gly has good crystallinity with a crystal size of 17.79 nm. MOF Cr-PTC-Gly with 50% glycine gave the most optimum elimination activity with an elimination capacity of 87.95 mg/gram via adsorption and photocatalytic degradation. The adsorption mechanisms were carried out via electrostatic interaction, hydrogen bonding, and π-π interaction. In contrast, photocatalytic degradation was carried out by forming free radical species with hydroxyl radicals (•OH) as a dominant species that contributed to the methylene blue degradation.

Keywords : Glycine, Methylene blue, MOF Cr-PTC-Gly, photocatalytic degradation

INTRODUCTION

Metal-organic frameworks (MOFs) are the most widely developed semiconductor materials for dye removal applications. For their advantages, MOFs are applied as photocatalysts, including flexibility, porous crystalline material, large surface area, and uniform active site distribution (Kaur et al., 2019). Metal-organic frameworks (MOFs), one of the semiconductor materials, were developed to overcome the limitation of metal oxide-based semiconductors like large band gaps energy. It is due to the band gap energy of MOFs can be tuned by using an appropriate metal ion and linker. Studies reported metal-organic frameworks (MOFs) materials for dye elimination applications. Yudanto (2018) synthesized a La-MOF-based linker of benzene-1,4-dicarboxylic acid (BDC) with an band gap energy of 3.61 eV for Rhodamine B degradation under UV light irradiation. Then, Batubara (2019) reported an organic linker-based La-MOF naphthalene-2,6-dicarboxylic acid (NDC) with an band gap energy of 3.1 eV for Rhodamin degradation under UV light irradiation. Zulys et al. (2021) also synthesized La-MOFs based on organic ligand perylene-3,4,9,10-tetracarboxylic dianhydride

(PTCDA) with an energy band gap of 2.25 eV for methylene blue degradation under visible light irradiation. Of those three organic ligands, PTCDA is the one able to increase the photosensitivity of MOFs to visible light radiation.

However, MOFs still have limitations in practical application due to the rapid electron-hole recombination effect that reduces their catalytic activity (Syzgantseva et al., 2019). A strategy to overcome this problem is adding a modulator like glycine, proline, phenylalanine, and benzoic acid (Chambers et al., 2017; Gutov et al., 2016; Hasan, 2015). Adding an amino acid modulator can produce MOFs with high crystallinity, small particle sizes, and high porosity as desired in dye catalytic photodegradation. In addition, amino acids can also cover structural defects of elements (Gutov et al., 2016).

Gutov et al. (2016) synthesized amino acid-modulated Zr-MOF that produced high porosity MOF and reduced the crystal defects that were the main factors causing recombination. Then, Dong et al. (2017) reported that the addition of glycine as a modulator increases the catalytic activity and stability

of MOF MIL-53 (Fe) due to the ability of carboxylate and amine functional groups to bind metal ions.

Therefore, this study aims to synthesize novel visible active glycine-modulated MOF-based chromium metal ion and perylene-3,4,9,10-tetracarboxylic dianhydride organic linker for methylene blue under visible light irradiation.

EXPERIMENTAL SECTION
Materials

The chemicals for this research are chromium(III) chloride hexahydrate ($CrCl_3.6H_2O$) (Merck), sodium hydroxide (NaOH) (Merck), Perylene 3,4,9,10-tetracarboxylic dianhydride (PTCDA) (Sigma-Aldrich), N,N-dimethyl-formamide (DMF) (Loba Chemie PVT.LTD), glycine (Merck), ethanol (C_2H_5OH) (Merck), methylene blue (Merck), distilled water (H_2O), hydrogen peroxide (H_2O_2) (Merck), tertier butanol (tert-BuOH) (Merck), methanol (CH_3OH) (Merck), $BaSO_4$ (Merck), and potassium bromide (KBr) (Merck).

Preparation of Na₄PTC (Zulys et al., 2021)

PTCDA (0.5 g; 1.27 mmol) was dissolved with 50 mL of distilled water, then added with NaOH (0.356 g; 8.9 mmol) while magnetically stirred for one hour at 300 rpm. Then, the greenish orange suspension was filtered. Next, the filtrate was added with excess ethanol to get a yellow precipitate. Furthermore, the yellow Na_4PTC precipitate was filtered and washed with ethanol until the pH of the filtrate was neutral. Finally, the yellow Na_4PTC precipitate was dried at room temperature overnight.

Synthesis MOFs Modulated Glycine (Cr-PTC-Gly)

The synthesis of Cr-PTC was carried out using a solvent mixture of distilled water (H_2O) and N,N-dimethyl formamide (DMF) (5:1) as much as 30 mL. Chromium(III) chloride (0.265 g; 1 mmol) and Na_4PTC (0.258 g; 0.5 mmol) were dissolved with DMF and H_2O mixture. Next, the mixture was magnetically stirred at 300 rpm for one hour. Then it was transferred to the Teflon-lines autoclave and heated at 170 °C for 24 hours. The mixture was cooled at room temperature overnight. The red-brown precipitate was filtered and washed with distilled water. Finally, the precipitate was dried for 24 hours at 70 °C overnight.

Cr-PTC-Gly was prepared by stirring 0.2 g of Cr-PTC and glycine (40; 50 and 60% b/b) in 100 mL of distilled water for an hour at 300 rpm. Then, the mixture was heated for 24 hours at 50 °C. Finally, the red-brown powder formed was filtered and washed with distilled water and dried at 70 °C for 24 hours.

Characterization of MOF Cr-PTC-Gly

The MOF Cr-PTC was characterized by X-Ray diffraction spectroscopy (7000 Maxima-X) for crystallinity and crystal size analysis. FTIR (Prestige 21 Shimadzu) for determining the functional groups, UV-Vis DRS Spectrophotometer Agilent Carry 60 for measuring the band gap energy at 200-800 nm wavelength with $BaSO_4$ as a reference.

Methylene Blue Elimination Analysis

The methylene blue elimination was measured by dispersing 25 mg of MOFs Cr-PTC-Gly into 50 mL of methylene blue (50 mg/L) and then magnetically stirred at 300 rpm at room temperature for three hours in the dark and under 250 watts of mercury lamp irradiation as a visible light source. Furthermore, the suspension was sampled as much as 2.0 mL every 30 minutes, then centrifuged at 6000 rpm for 10 minutes. The methylene blue concentration was measured using a UV-Vis spectrophotometer at 665 nm. The methylene blue elimination percentage is calculated using equation 1.

$$\text{Elimination (\%)} = \frac{(C_o - C_t)}{C_o} \times 100\% \qquad (1)$$

Where C_o is the initial concentration, and C_t is the final concentration.

The optimum condition was measured by using several parameters, including the concentration of glycine, initial methylene blue concentration (25, 50, and 75 ppm), MOF Cr-PTC-Gly dosage (15, 25, 35, and 45 mg), and initial of pH (2, 5, 7, 9 and 11). A fixed amount of sacrificial agents like H_2O_2, CH_3OH, and a mixture of H_2O_2 and tert-BuOH was added to determine the dominant species in the methylene blue photocatalytic degradation.

RESULT S AND DISCUSSION
Natrium Perylene 3,4,9,10-tetracarboxylate (Na₄PTC)

Figure 1 shows the IR spectra of PTCDA and Na_4PTC. In the PTCDA spectrum, there is a sharp absorbance peak at 1772 cm^{-1}, which indicates the functional group of the 5-member PTCDA cyclic anhydride compound. The bands at 1753 and 1730 cm^{-1} attributed to asymmetric and symmetric stretching vibrations (C=O) of PTCDA 5-member ring cyclic anhydride. The sharp peak at 1234 cm^{-1} confirmed asymmetric stretching vibration (C-O), and 938 cm^{-1} identified the symmetric stretching vibration (C-O) of the C-CO-O-CO-C- group in the cyclic anhydride compound of PTCDA (Adawiah et al., 2021). Figure 1 also shows that the five bands of the cyclic anhydride group of the PTCDA no longer appear in the IR spectrum of Na_4PTC. In addition, the IR spectrum of Na_4PTC showed new bands at 1633 and 1423 cm^{-1}, which identified asymmetric and symmetric stretching vibrations of the (-COO) group carboxylate ion. These new bands indicate that PTCDA forms a carboxylate ion with sodium ions derived from NaOH. At 2500-3300 cm^{-1} in the IR spectrum of Na_4PTC, no absorbance band was found for the -OH group. It confirmed that PTCDA reacts completely with four equivalents of NaOH to form Na_4PTC (Adawiah et al., 2021).

Characteristics of Metal Organic Framework (MOF) Cr-PTC-Gly

The IR spectra of MOFs Cr-PTC-Gly showed sharp absorbance in wavenumbers at around 1650-1500 cm^{-1}, 1440-1380 cm^{-1}, and 900-657 cm^{-1} (Figure 2). The IR spectrum of Na_4PTC showed asymmetric and

symmetric stretching (-COO) vibrations at 1633 cm^{-1} and 1423 cm^{-1}. There is a shift in the MOFs Cr-PTC-Gly to the wavenumber of 1506 and 1406 cm^{-1}, which were asymmetric and symmetrically stretching vibrations (-COO) bound to the Cr^{3+} ion. It explained that the (-COO) ion is no longer bound to Na$^+$ but has coordinated with the Cr^{3+} metal ion. The peak at 3118 cm^{-1} confirmed a hydroxyl (OH) functional group (Senthil et al., 2013).

The absorbance peak at 2034 cm^{-1} identified the stretching vibration N-H originating from glycine compounds (Kishor et al., 2013). Characteristics of the aromatic ring of perylene in MOFs Cr-PTC-Gly showed the presence of a sharp absorbance band at 1590 cm^{-1}, which shows an aromatic stretching vibration (C-C=C). The peak at 1406 cm^{-1} confirmed the weak peak of symmetric stretching vibration (-COO). Furthermore, the bending vibrations (C-H) in-plane aromatic rings in the three absorbance bands at 1233, 1119, and 1015 cm^{-1}. In addition, the absorbance peaks at 857 and 806 cm^{-1} show bending vibrations (C-H) out of planes 1,2,3,4-tetrasubstituted aromatic rings, and absorbance peaks at 757 and 730 cm-1 show out of the plane. Then, the peak at 528 cm^{-1} is the Cr-O strain vibration. The Cr-O strain vibration proves that the synthesis of Cr-PTC-Gly MOF is complete, where the metal cluster binds to the PTC carboxylate group (Seikh et al., 2019).

Figure 3 exhibits that MOF Cr-PTC and Cr-PTC-Gly have good crystallinity and the same diffractogram pattern with sharp spectral peaks at 2θ = 9.2°; 12.84°; 25.58°; and 27.805°. The Debye Scherer equation obtained a crystal size of Cr-PTC and Cr-PTC-Gly is 17.57 nm and 17.79 nm, respectively. It indicates that modulated glycine to Cr-PTC did not change the crystal structure of Cr-PTC.
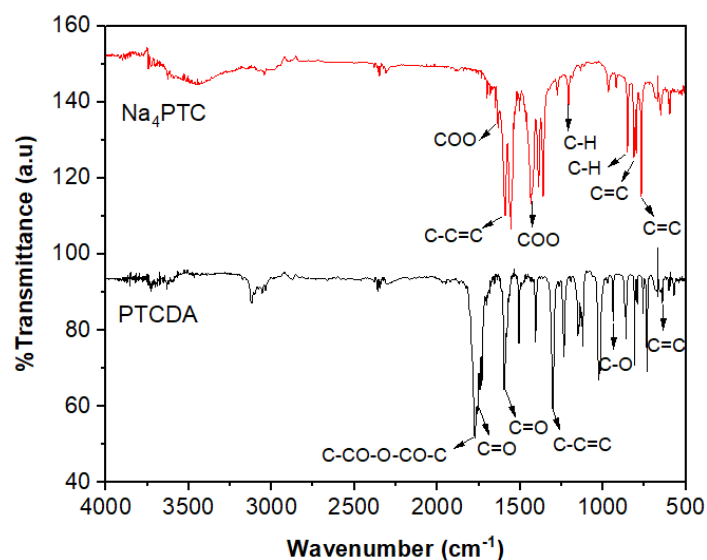
Figure 1. IR spectrum of PTCDA and Na$_4$PTC
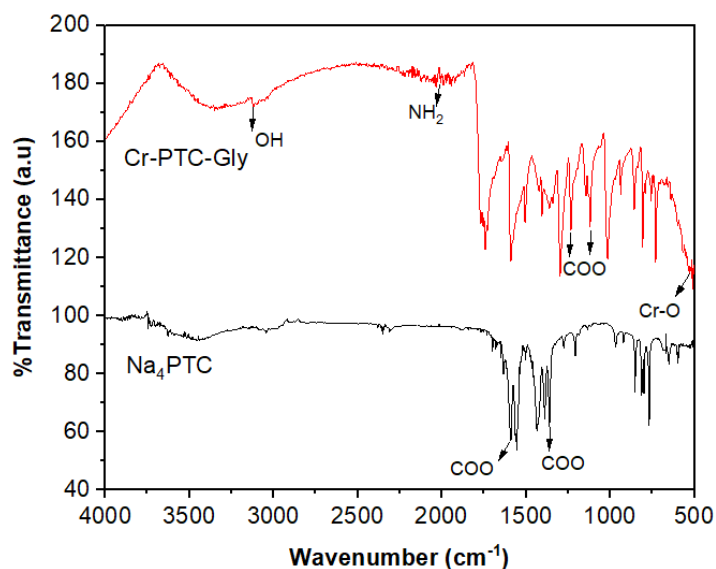
Figure 2. IR spectrum of MOFs Cr-PTC-Gly and Na$_4$PTC

Kudo and Miseki (2009) explained that the crystal structure affects the photocatalytic reaction. The high crystallinity of materials leads to small crystal defects. Crystal defects act as trapping and recombination centres of electron-hole pairs and generate reducing photocatalytic activity. Therefore, the recombination can be inhibited by a high crystallinity photocatalyst material.

The UV-Vis diffuse reflectance spectroscopy (DRS) analysis was employed to determine the band gap energy using the Kulbelka-Munk equation combined with the Tauc plot. The band gap energy is the energy between the valence band (VB) and the conduction band (CB) proportional to the energy required for electrons to be excited from the valence band to the conduction band. **Figure 4** revealed that the band gap energy (Eg) of the Cr-PTC-Gly is 1.9 eV, indicating that the Cr-PTC-Gly is a visible light responsive semiconductor material with an absorbance wavelength of 652 nm.

The organic linker, chromium metal ion, and glycine affected the Cr-PTC-Gly low band gap energy. Na_4PTC is a perylene-based organic linker with five aromatic rings. The number of conjugated bonds of the aromatic ring contributes to the low band gap energy value or high responsiveness to visible light. Yudanto (2018) synthesized La-MOF based on organic linker BDC (1,4-benzene dicarboxylic acid) with a band gap energy (Eg) of 3.61 eV. Subsequently, Batubara (2019) synthesized La-MOF based on the organic linker 2,6-naphthalene dicarboxylate (NDC) with a band gap energy (Eg) of 3.1 eV. Then, Zulys et al., (2021) synthesized La-MOF based on the organic linker Na_4PTC with an energy band gap (Eg) of 2.25 eV. It Exhibits that the perylene-based organic linker (Na_4PTC) produced MOFs with the most negligible band gap energy among the other two organic linkers. It is due to the influence of the π-π* electronic transition on the conjugated bond of a perylene ligand. The higher the conjugated bonds, the greater the electronic transition effect.
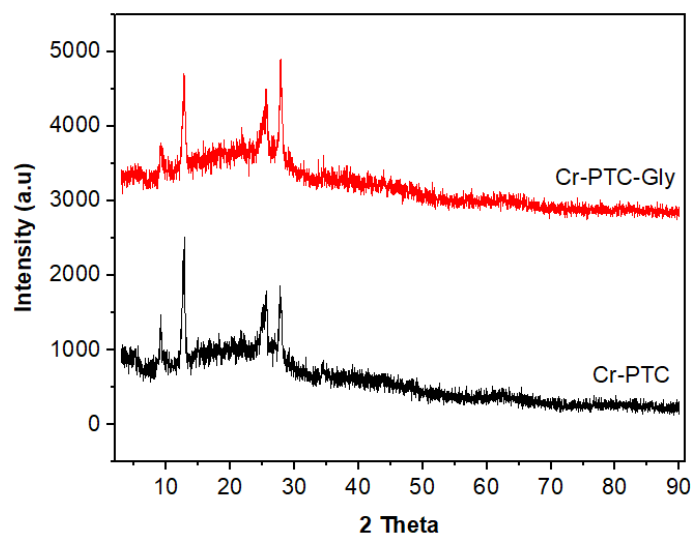
Figure 3. XRD diffractogram pattern of Cr-PTC and Cr-PTC-Gly.

(a)

(b)
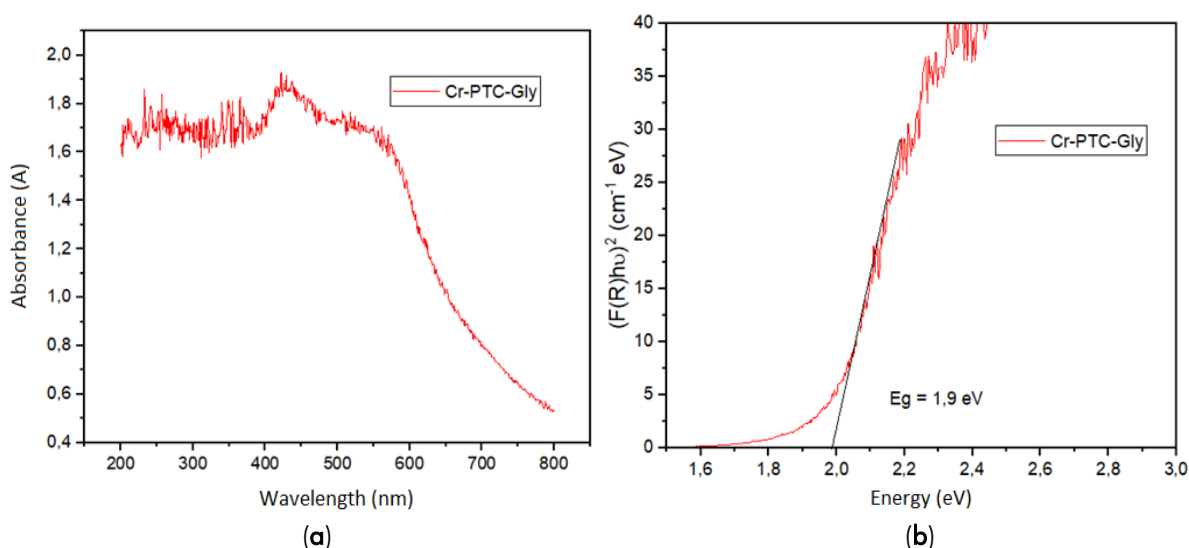
Figure 4. Reflectance spectrum (**a**) and energy band gap of Cr-PTC-Gly (**b**)

On the other hand, chromium metal ion (Cr^{3+}) applied to MOF Cr-PTC-Gly is a partially filled d orbital-transition metal. It has an essential role in the responsiveness toward visible light. Zulys et al. (2021) reported lanthanum metal ion-based La-PTC with an band gap energy of 2.25 eV, which is higher than Cr-PTC of 2.01 eV (previous study). The Eg value of MOFs-based semiconductors can be tuned by adjusting the metal atom's secondary building unit (SBU). The structure of MOFs is composed of ligand-SBU interface interactions so that ligand-SBU interface interactions influence the MOF's electronic properties. Increasing the size of SBU caused a narrowing of the band gap energy (Eg) of MOFs. The difference in the size of the SBU of the metal used provides a shift in the band gap energy of MOFs (Lin et al., 2012). The size of the SBU cluster increases with the number of electrons. Due to the increasing electron number in an element producing more electrons in the HOMO energy level. It is generating the band gap energy becomes narrow (Yang et al., 2012).

Besides that, adding glycine to the Cr-PTC reduces the energy band gap. The glycine modulator has a -NH_2 functional group that acts as an energy band gap control. The -NH_2 group replaces the hydrogen atom in the MOFs to form an interaction that disrupts the electron density distribution of the MOFs and will affect the band gap energy (Flage et al., 2013). Li et al., (2018) succeeded in synthesizing MIL-125 with BDC linker producing MOFs with an band gap energy of 4.08 eV. After adding the amine group to form NH_2-MIL-125, the band gap energy decreased to 2.68 eV.

Methylene Blue Elimination

Methylene blue elimination by MOF Cr-PTC-Gly was carried out under dark and visible light irradiation. MB elimination measuring in the dark aims to determine the adsorption ability of Cr-PTC-Gly in MB elimination. MOFs are porous materials that can eliminate dyes through an adsorption mechanism (Zulfa et al., 2019). **Figure 5** shows all MOF Cr-PTC-Gly eliminate MB in the dark with an elimination percentage of 42.22; 31.93; and 31.82% for 180 minutes of incubation. The adsorption of MB

molecules by MOF occurs through several interaction mechanisms (adsorbate-adsorbent), including electrostatic, acid-base, hydrogen bonds, π-π interactions, hydrophobic interactions, or a combination of these interactions (Hasan & Jhung, 2015).

MB adsorption process by Cr-PTC-Gly is affected by several interactions, including electrostatic interactions, π-π interactions, and hydrogen bond interactions. Electrostatic interaction occurs when charged MOFs readily interact with oppositely charged adsorbates. Hasan and Jhung (2015) explained that electrostatic interactions occur between positively charged MB on the nitrogen (N) or sulfur (S) atoms that interact with the negative charge of the benzene ring in MOF. The following interaction is the π-π interaction that occurs when the aromatic ring in the MB structure interacts with the aromatic ring of the perylene linker used in Cr-PTC-Gly. Another interaction is hydrogen bonds between hydrogen atoms (H) in MB with nitrogen atoms (N) from glycine in Cr-PTC-Gly. In addition, hydrogen bonding also occurs between the N atom in MB and the H atom in the NH_2 group of glycine in the Cr-PTC-Gly. The presence of these groups in the structure of MOF enhance the MOFs adsorption ability.

Figure 5 illustrates that Cr-PTC-Gly also has photocatalytic activity in MB degradation. There is an increasing MB elimination for MOF Cr-PTC-Gly 40, 50, and 60% of 1.59, 21.22, and 12.44%, respectively. Increasing MB elimination by MOF Cr-PTC-Gly at 50% glycine had the most significant photocatalytic activity. Besides that, Cr-PTC-Gly 50% has higher MB removal than Cr-PTC without modulation with the removal percentage of 52.31% and 48.38%, respectively (previous study). Photocatalytic activity of MOFs Cr-PTC-Gly (40%) is the lowest degradation efficiency. It is due to MOF Cr-PTC-Gly (40%) having very high adsorption. MB molecules were adsorbed too much to cover the photocatalyst surface. It caused the incoming light not to penetrate the MOFs surface, which inhibited electron excitation, and the photocatalytic reactions are challenging to achieve (Kuang et al., 2020).
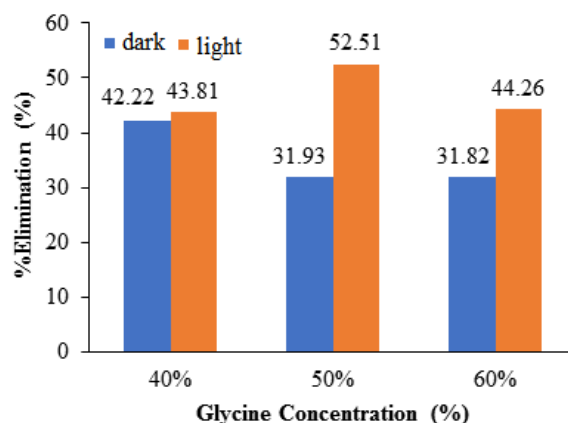
Figure 5. Methylene blue elimination by MOF Cr-PTC-Gly under dark and light condition

However, at the concentration of 60%, there was a decrease in elimination percentage. It is due to the concentration of glycine added was excessive. The excess glycine generates the competition between Na_4PTC and glycine. Thus, the formation of crystalline solids Cr-PTC-Gly is increasingly tricky, and large crystal sizes are obtained. Wang et al. (2013) fabricated HKUST-1 modulated sodium formate with concentrations of 30% and 50% with crystal sizes of 100 nm and 115 nm, respectively.

Effect of MOF Cr-PTC-Gly Dosage

Figure 6 shows MOF Cr-PTC-Gly dosage of 5 mg exhibited a small elimination of 20.63% because the MOF dosage dispersed was too small. The MB molecules covering the active site on the MOFs' surface inhibited light penetration and decreased the methylene blue photocatalytic degradation. Meanwhile, the Cr-PTC-Gly dosage of 15 mg and 25 mg performed the increasing MB elimination. **Figure 6** revealed that the Cr-PTC-Gly dosage of 25 undergoes a significant elimination rate than the 15 mg, resulting in an elimination percentage of 87.95%. The increasing MOF dosage causes more active sites used for MB elimination.

Simultaneously, MOF Cr-PTC-Gly dosages of 35 and 45 mg showed the high percent elimination for the first 30 minutes. However, at 180 minutes, the photocatalytic activity of 45 mg of MOF was smaller than 35 mg (**Figure 6**). The MOF dosage of 45 mg enhances the solution turbidity due to the Cr-PTC-Gly particles exceeding the optimum limit that cause agglomeration to form colloids. In addition, it contributed to the lowering of penetrating photons in the system. Chiu et al. (2019) explained that adding an excess photocatalyst dosage makes the solution cloudy. It prevents light penetration to the photocatalyst and inhibits the excited electron formation that plays a role in MB degradation.
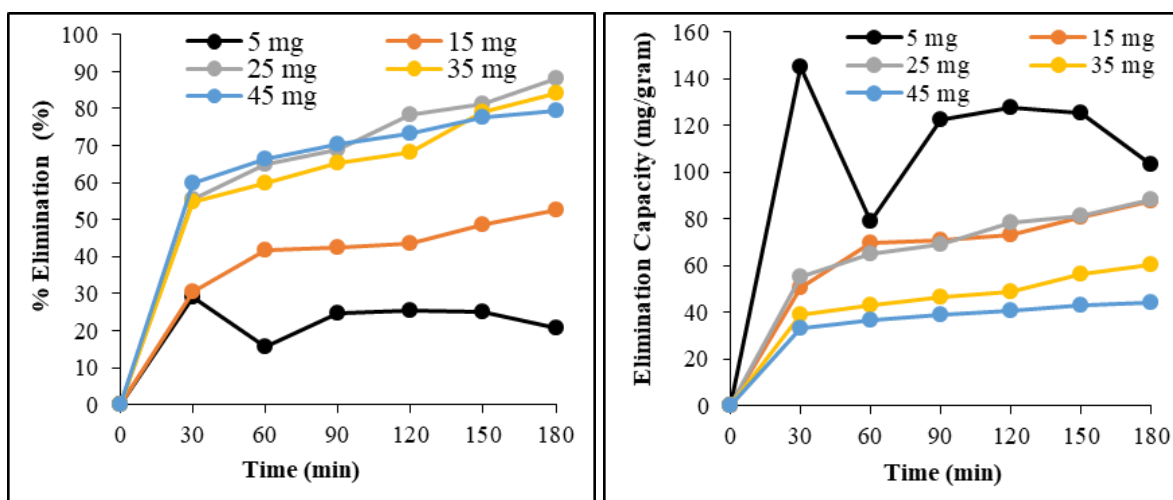
Effect of Initial Methylene Blue Concentration

Figure 7 shows the percent elimination of methylene blue at MB initial concentration of 25 ppm is 92.48% for 180 minutes. Meanwhile, at 50 ppm and 75 ppm, methylene blue was only degraded by 87.95 and 29.87% at the same time. However, MOF Cr-PTC-Gly had the largest elimination capacity of 87.95 mg/gram in initial MB concentration of 50 ppm than of 25 ppm and 75 ppm, resulting in elimination capacity of 46.47 mg/gram and 44.80 mg/gram, respectively.

In contrast to the initial concentration of 75 ppm, percent elimination and elimination capacity were decreased. Due to an initial methylene blue concentration of 75 ppm, the elimination of methylene blue occurred via the adsorption process. The more significant MB molecule covers the active site of the MOF's surface, which decreases light penetration power. In addition, it inhibits the electron excitation process, reduces electron-hole pairs formation, and discourages radicals ($\bullet OH$) and superoxide radicals ($\bullet O_2^-$) which contribute to photocatalytic oxidizing dyes (Abdellah et al., 2018).

The Effect of pH

Jing et al., (2014) explained that the pH of the solution is one of the critical parameters affecting photocatalytic degradation. It is because pH influences the stability of a photocatalyst. Figure 8 exhibited under acidic conditions at pH 2 and 5 the methylene blue elimination of 0.59 and 3.10% with an elimination capacity of 0.59 and 3.10 mg/gram, respectively. Then, at pH 7 (neutral), a percent elimination of 87.95% with an elimination capacity of 87.95 mg/gram. Furthermore, at pH 9 and 11 (alkaline conditions), the percent elimination was 82.53 and 85.07%, respectively, with an elimination capacity of 82.53 and 85.07 mg/gram.

Figure 6. The methylene blue percent elimination and elimination capacity in various MOF Cr-PTC-Gly dosage
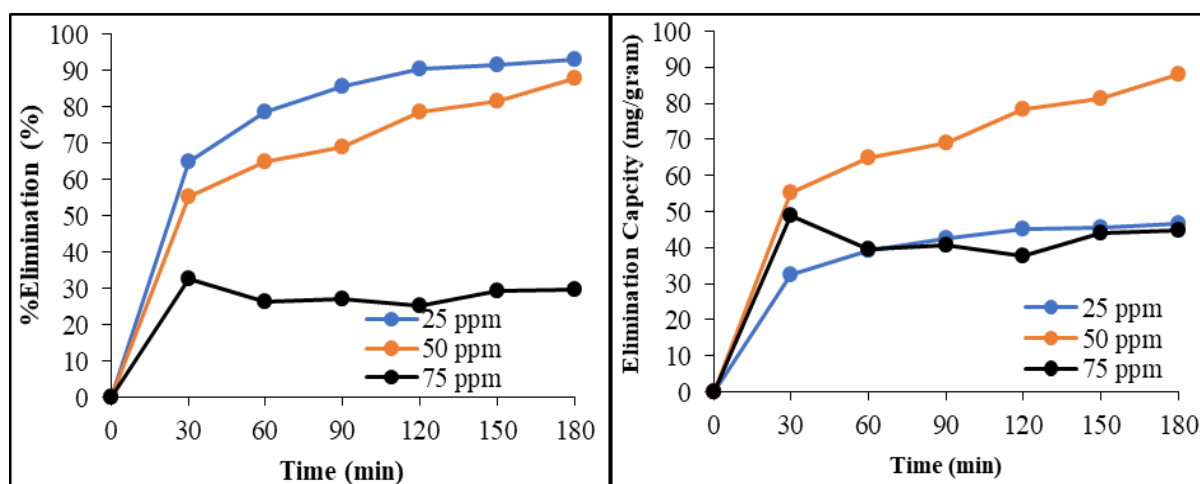
Figure 7. The methylene blue percent elimination and elimination capacity in various of methylene blue degradation
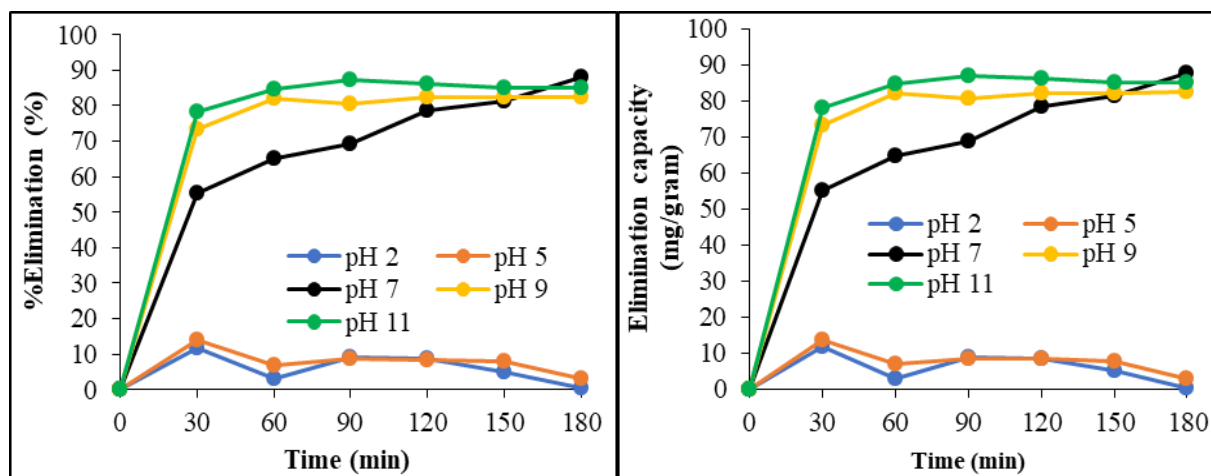
Figure 8. The methylene blue percent elimination and elimination capacity in various pH

MOF Cr-PTC-Gly did not have photocatalytic activity in acidic conditions (pH 2 and 5). In a low pH (acidic) environment, an excess of H^+ ions decreases the number of hydroxyl radicals ($\bullet OH$) that play a role in the degradation process. Excess H^+ ions will interact with excited electrons (e^-) to form $\bullet H$ radicals which can react back with $\bullet OH$ radicals to form H_2O. The reaction mechanism under acidic conditions follows Equation 2-5 (Nasikhudin et al., 2018).

$$MOF + h\nu \rightarrow MOF~(e_{cb}^- + h_{vb}^+) \qquad (2)$$
$$h_{vb}^+ + H_2O \rightarrow H^+ + \bullet OH \qquad (3)$$
$$H^+ + e_{cb}^- \rightarrow \bullet H \qquad (4)$$
$$\bullet H + \bullet OH \rightarrow H_2O \qquad (5)$$
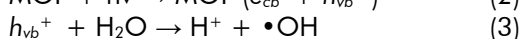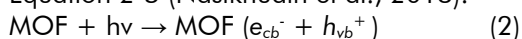
In addition, at pH 2 and 5, the adsorption ability of Cr-PTC-Gly on MB was deficient. The excess H^+ ions will protonate the negative charge on the MOFs, so the MOFs tend to be less negatively charged. Methylene blue is a cationic dye. If the MOFs tend to be less negative, then the electrostatic interaction between MOFs and MB will be weak, and it will reduce the adsorption capacity of MOFs. It is also reinforced by the condition where pH 2 produces lower elimination percentage than pH 5 because the number

of H^+ ions at pH 2 is more than at pH 5 (Paiman et al., 2020).

In contrast to acidic conditions, under pH 9 and 11, the percent elimination was quite large under alkaline conditions, namely 82.53% and 85.07%, respectively. Under alkaline conditions, Cr-PTC-Gly MOFs did not have photocatalytic activity. It can be seen from the insignificant change in the elimination capacity. Under the alkaline condition, MB elimination only occurs through the adsorption mechanism. At alkaline conditions, the MOFs' surface deprotonated. As a result, the number of negatively charged sites increased due to the presence of OH^- ions. It caused the MOFs surface to be more positively charged and the electrostatic interactions to become stronger (Lim et al., 2021). The adsorption of pH 9 was lower than that of pH 11 because at pH 11, the number of OH^- ions increased, and the MOF tended to be significantly negatively charged, resulting in increased electrostatic bonds (Firoozi et al., 2020). In addition, the absence of photocatalytic activity under alkaline conditions due to the Cr-PTC-Gly MOF was unstable, causing damage to their structure. It is evidenced by the

change in the colour of the solution from blue to green. Cr-PTC-Gly MOF is made of high valence chromium metal ion (+3 charge) and carboxylate-based ligands. Therefore, Cr-PTC-Gly has high stability in acidic and neutral conditions, not under alkaline conditions (Yuan et al., 2018). The addition of NaOH solution originated the decomposition of MOFs Cr-PTC-Gly into water-soluble chromium(III) hydroxide $(Cr_3OH)_6^{3-}$, which is indicated by a change in the colour of the green solution. The decomposition reaction occurred by exchanging the carboxylate (COO-) ligand with the OH- (equations 6 and 7).

$$M^{HV} – (OOCR^-) + OH^- → M^{HV}\text{-}OH^- + RCOO^- \quad (6)$$
$$Cr–PTC\text{-}Gly_{(s)} + OH^-_{(aq)} → Cr(OH)_6^{3-}{}_{(aq)} + \\ PTC^- + Gly \quad (7)$$
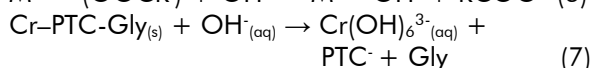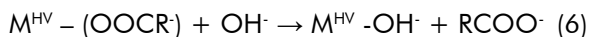
Methylene Blue Photocatalytic Degradation Mechanism by Cr-PTC-Gly

Figure 9 shows the photocatalytic activity Cr-PTC-Gly after adding an electron-hole scavenger, like hydrogen peroxide (H_2O_2), methanol, and a mixture of H_2O_2 and tert-BuOH with an elimination percentage of 90.39%, 53.13%, and 87.90%, respectively. In the presence of H_2O_2, MB elimination percentage increases from 87.90% to 90.39%. H_2O_2 acts as an electron-scavenger that prevents the recombination of excited electron (e-) and electron holes (h+) pairs. H_2O_2 reacts with excited electrons to produce hydroxide ions (OH-) and hydroxyl radicals (•OH) (Wang et al., 2014). In addition, the added H_2O_2 was also decomposed by light to produce hydroxyl radicals (•OH). Therefore, H_2O_2 employs increasing •OH radicals, which play an essential role in MB degradation. Equation 8-12 shows the mechanism of the photocatalytic degradation of dyes in H_2O_2 (Fakhrul et al., 2018).

$$MOF + hv → MOF (e\bar{c}_B + h_v^+{}_B) \quad (8)$$
$$e\bar{c}_B + H_2O_2 → •OH + OH^- \quad (9)$$

$$H_2O_2 + light (hv) → •OH + OH^- \quad (10)$$
$$h_v^+{}_B + OH^- → •OH \quad (11)$$
$$h_v^+{}_B + H_2O → •OH \quad (12)$$
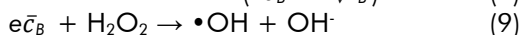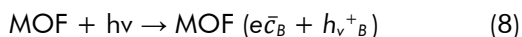
The addition of methanol as a hole (h+) trapping agent ensued an elimination percentage of 53.77% for 180 minutes, which was smaller than the elimination percentage without methanol of 87.95%. When methanol is added to the system, the holes (h+) in the conduction band will oxidize methanol to hydroxyalkyl radicals (•CH2-OH) and further oxidize to formaldehyde (CH2O). Thus, the hydroxyl radicals (•OH) from the reaction between electron holes and water, is not formed. However, the photoexcited electrons will react with oxygen to form superoxide radicals (•O2-). Superoxide radicals (•O2-) have lower strength than hydroxyl radicals. Therefore, the MB degradation efficiency with methanol presence is lower than that. The equation 13-15 shows the MB dye degradation by Cr-PTC-Gly in methanol.

$$MOFs + hv → MOFs (e_{cb}^- + h_{vb}^+) \quad (13)$$
$$h_{vb}^+ + CH_3OH → •CH_2OH → CH_2O \quad (14)$$
$$e_{cb}^- + O_2 → •O_2^- \quad (15)$$
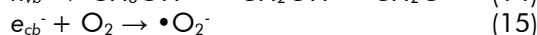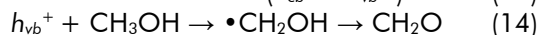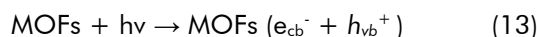
The elimination percentage was decreased from 90.39% to 87.90% in the presence of H_2O_2 and tert-butanol mixture. It indicated that free radical species (•OH) contributed significantly to photocatalytic MB degradation. It is due to the decreasing •OH radical species number emerged due to being captured by the tert-BuOH molecule. The MB degradation by Cr-PTC-Gly in the presence of tert-BuOH and H_2O_2 was explained by equations 16-20.

$$MOF + hv → MOF (e_{cb}^- + h_{vb}^+) \quad (16)$$
$$e_{cb}^- + H_2O_2 → •OH + OH^- \quad (17)$$
$$h_{vb}^+ + OH^- → •OH \quad (18)$$
$$h_{vb}^+ + H_2O → •OH \quad (19)$$
$$(CH_3)_3COH + •OH → (CH_3)_3CO + H_2O \quad (20)$$
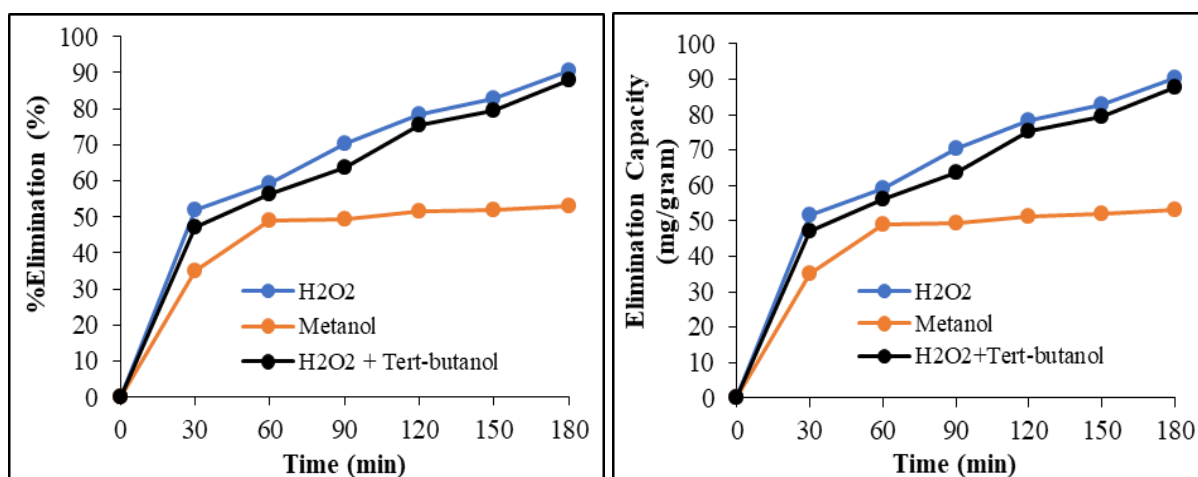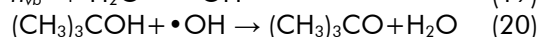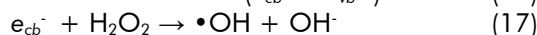
Figure 9. The methylene blue percent elimination and elimination capacity in the addition of electron-hole scavenger

CONCLUSIONS

This research has succeeded in synthesizing glycine-modulated Cr-metal organic framework MOF Cr-PTC-Gly. The MOF Cr-PTC-Gly eliminates methylene blue through adsorption and photocatalytic mechanisms under neutral pH conditions with a elimination capacity of 87.95 mg/gram for 180 minutes of reaction time. The adsorption mechanisms were carried out via electrostatic interaction, hydrogen bonding and π-π interaction. While the photocatalytic degradation mechanism was carried out via free radical species formation with hydroxyl radicals ($\bullet$OH) as dominant species in MB degradation.

ACKNOWLEDGMENTS

REFERENCES

Abdellah, M. H., Nosier, S. A., El-Shazly, A. H., & Mubarak, A. A. (2018). Photocatalytic decolorization of methylene blue using TiO2/UV system enhanced by air sparging. *Alexandria Engineering Journal*, 57(4), 3727–3735. https://doi.org/10.1016/j.aej.2018.07.018

Adawiah, A., Yudhi, M. D. L., & Zulys, A. (2021). Photocatalytic degradation of methylene blue and methyl orange by Y-PTC metal-organic framework. *Jurnal Kimia Valensi*, 7(2), 129–141. https://doi.org/10.15408/jkv.v7i2.22267

Batubara, N. H. (2019). Sintesis metal organic frameworks dengan logam lantanum (III) dan ligan 2,6-naftalendikarboksilat (La-MOFs) sebagai fotokatalis penghasil gas hidrogen. (Synthesis of metal organic frameworks with lanthanum metal (III) and 2,6-naphthalendicarboxylate ligands (La-MOFs) as photocatalysts to produce hydrogen gas). Universitas Indonesia.

Chambers, M. B., Wang, X., Ellezam, L., Ersen, O., Fontecave, M., Sanchez, C., Mellot-Draznieks, C. (2017). Maximizing the Photocatalytic Activity of Metal-Organic Frameworks with Aminated-Functionalized Linkers: Substoichiometric Effects in MIL-125-NH2. *Journal of the American Chemical Society*, 139(24), 8222–8228. https://doi.org/10.1021/jacs.7b02186

Chiu, Y. H., Chang, T. F. M., Chen, C. Y., Sone, M., & Hsu, Y. J. (2019). Mechanistic insights into photodegradation of organic dyes using heterostructure photocatalysts. *Catalysts*, 9(5). https://doi.org/10.3390/catal9050430

Dong, W., Yang, L., & Huang, Y. (2017). Talanta Glycine post-synthetic modification of MIL-53 (Fe) metal-organic framework with enhanced and stable peroxidase-like activity for sensitive glucose biosensing. *Talanta*, 167(November 2016), 359–366. https://doi.org/10.1016/j.talanta.2017.02.039

Fakhrul R. S., M., Tau, S. L., Sufian, S., Bashiri, R., Muti M. N., & Mahirah R. R. (2018). Exploring the role of electron-hole scavengers on optimizing the photocatalytic performance of BiVO4. *Materials Today: Proceedings*, 5(10), 21703–21709. https://doi.org/10.1016/j.matpr.2018.07.022

Firoozi, M., Ra, Z., & Dashtian, K. (2020). New MOF/COF hybrid as a robust adsorbent for simultaneous removal of auramine O and rhodamine B dyes. *ACS Omega*. https://doi.org/10.1021/acsomega.0c00539

Flage L. E., Røyset, A., Cavka, J. H., & Thorshaug, K. (2013). Band gap modulations in UiO metal-organic frameworks. *Journal of Physical Chemistry C*, 117(40), 20610–20616. https://doi.org/10.1021/jp405335q

Gutov, O. V., Molina, S., Escudero-Adán, E. C., & Shafir, A. (2016). Modulation by amino acids: toward superior control in the synthesis of zirconium metal–organic frameworks. *Chemistry-A European Journal*, 22(38), 13582–13587. https://doi.org/10.1002/chem.201600898

Hasan, M. R. (2015). Pengaruh penambahan modulator asam asetat pada sintesis metal organic framework tipe HKUST-1 (Effect of adding acetic acid modulator on the synthesis of metal organic framework type HKUST-1). Institut Teknologi Sepuluh Nopember Surabaya.

Hasan, Z., & Jhung, S. H. (2015). Removal of hazardous organics from water using metal-organic frameworks (MOFs): Plausible mechanisms for selective adsorptions. *Journal of Hazardous Materials*, 283, 329–339. https://doi.org/10.1016/j.jhazmat.2014.09.046

Jing, H. P., Wang, C. C., Zhang, Y. W., Wang, P., & Li, R. (2014). Photocatalytic degradation of methylene blue in ZIF-8. *RSC Advances*, 4(97), 54454–54462. https://doi.org/10.1039/c4ra08820d

Kaur, H., Kumar, A., Koner, R. R., & Krishnan, V. (2019). Metal-organic frameworks for photocatalytic degradation of pollutants. In *Nano-Materials as Photocatalysts for Degradation of Environmental Pollutants: Challenges and Possibilities*. Elsevier Inc. https://doi.org/10.1016/B978-0-12-818598-8.00006-7

Kishor K. J., Gunasekaran, S., Loganathan, S., Anand, G., & Kumaresan, S. (2013). The molecular structure, geometry, stability, thermal and fundamental modes of vibration of glycine dimer by DFT methods. *Spectrochimica Acta -*

Part A: Molecular and Biomolecular Spectroscopy, *115*, 730–737. https://doi.org/10.1016/j.saa.2013.06.097

Kuang, Y., Zhang, X., & Zhou, S. (2020). Adsorption of methylene blue in water onto activated carbon by surfactant modification. *Water (Switzerland)*, *12*(2), 1–19. https://doi.org/10.3390/w12020587

Kudo, A., & Miseki, Y. (2009). Heterogeneous photocatalyst materials for water splitting. *Chemical Society Reviews*, *38*(1), 253–278. https://doi.org/10.1039/B800489G

Li, Y., Fu, Y., Ni, B., Ding, K., Chen, W., Wu, K., Zhang, Y. (2018). Effects of ligand functionalization on the photocatalytic properties of titanium-based MOF: A density functional theory study. *AIP Advances*, *8*(3). https://doi.org/10.1063/1.5021098

Lim, S., Kim, J. H., Park, H., Kwak, C., Yang, J., Kim, J., Lee, J. (2021). Role of electrostatic interactions in the adsorption of dye molecules by Ti3C2-MXenes. *RSC Advances*, *11*(11), 6201–6211. https://doi.org/10.1039/d0ra10876f

Lin, C. K., Zhao, D., Gao, W. Y., Yang, Z., Ye, J., Xu, T., Liu, D. J. (2012). Tunability of band gaps in metal-organic frameworks. *Inorganic Chemistry*, *51*(16), 9039–9044. https://doi.org/10.1021/ic301189m

Nasikhudin, Diantoro, M., Kusumaatmaja, A., & Triyana, K. (2018). Study on photocatalytic properties of TiO_2 nanoparticle in various pH condition. *Journal of Physics: Conference Series*, *1011*(1). https://doi.org/10.1088/1742-6596/1011/1/012069

Paiman, S. H., Rahman, M. A., Uchikoshi, T., Abdullah, N., Othman, M. H. D., Jaafar, J., Ismail, A. F. (2020). Functionalization effect of Fe-type MOF for methylene blue adsorption. *Journal of Saudi Chemical Society*, *24*(11), 896–905.
https://doi.org/10.1016/j.jscs.2020.09.006

Senthil K. R., Senthil K. S., & Anbu K. M. (2013). Efficient electrosynthesis of highly active $Cu_3(BTC)$ 2-MOF and its catalytic application to chemical reduction. *Microporous and Mesoporous Materials*, *168*, 57–64. https://doi.org/10.1016/j.micromeso.2012.09.028

Sheikh A. M., Hossein T, N. H. M., Shafiei-Alavijeh, M., Rashidi, A., Kooti, M., Pourreza, A., & Fakhraie, S. (2019). Synthesis of a modified HF-free MIL-101(Cr) nanoadsorbent with enhanced H_2S/CH_4 , CO_2/CH_4, and CO_2/N_2 selectivity. *Journal of Environmental Chemical Engineering*,

7(2). https://doi.org/10.1016/j.jece.2019.102946

Syzgantseva, M. A., Stepanov, N. F., & Syzgantseva, O. A. (2019). Carrier Lifetimes and Recombination Pathways in Metal-Organic Frameworks [Rapid-communication]. *Journal of Physical Chemistry Letters*, *10*(17), 5041–5046. https://doi.org/10.1021/acs.jpclett.9b02051

Wang, C. C., Li, J. R., Lv, X. L., Zhang, Y. Q., & Guo, G. (2014). Photocatalytic organic pollutants degradation in metal-organic frameworks. *Energy and Environmental Science*, *7*(9), 2831–2867. https://doi.org/10.1039/c4ee01299b

Wang, F., Guo, H., Chai, Y., Li, Y., & Liu, C. (2013). The controlled regulation of morphology and size of HKUST-1 by "coordination modulation method." *Microporous and Mesoporous Materials*, *173*, 181–188. https://doi.org/10.1016/j.micromeso.2013.02.023

Yang, L. M., Ravindran, P., Vajeeston, P., & Tilset, M. (2012). Ab initio investigations on the crystal structure, formation enthalpy, electronic structure, chemical bonding, and optical properties of experimentally synthesized isoreticular metal-organic framework-10 and its analogues: M-IRMOF-10 (M = Zn, Cd, Be, Mg, . *RSC Advances*, *2*(4), 1618–1631. https://doi.org/10.1039/c1ra00187f

Yuan, S., Feng, L., Wang, K., Pang, J., Bosch, M., Lollar, C., Zhou, H. C. (2018). Stable metal–organic frameworks: design, synthesis, and applications. *Advanced Materials*, *30*(37), 1–35. https://doi.org/10.1002/adma.201704303

Yudanto, R. W. (2018). Studi sintesis metal organic frameworks (mofs) dengan logam lantanum dan logam yttrium dan ligan BDC (1,4-benzene dicarboxyclic acid) sebagai fotokatalis degradasi dye rhodamin-B (Study on the synthesis of metal organic frameworks (mofs) with lanthanum metal and yttrium metal and BDC ligand (1,4-benzene dicarboxyclic acid) as photocatalyst for rhodamine-B dye degradation). Universitas Indonesia.

Zulfa, L. L., Ediati, R., & Kusumawati, Y. (2019). Sintesis MOF biner UiO-66 / HKUST-1. *Jurnal Sains Dan Seni ITS*, *8*(1), 8–10.

Zulys, A., Adawiah, A., Gunlazuardi, J., & Yudhi, M. D. L. (2021). Light-harvesting metal-organic frameworks (MOFs) La-PTC for photocatalytic dyes degradation. *Bulletin of Chemical Reaction Engineering & Catalysis*, *16*(1), 170–178. https://doi.org/10.9767/bcrec.16.1.10309.170-178